Polyhedron 252 (2024) 116877

Contents lists available at ScienceDirect

Polyhedron

journal homepage: www.elsevier.com/locate/poly

Dispersion energy donor ligand supports the isolation of Ge(II), Sn(II), and Lewis-base free Pb(II) arylthiolate dimers $\{M(SC_6H_2\text{-}2,4,6\text{-}Cy_3)_2\}_2$ (M = Ge, Sn, Pb; Cy = cyclohexyl)

Connor P. McLoughlin [a], Anthony J. Witt [a], Jonah P.D. Nelson [b,c], Heikki M. Tuononen [b,*], Philip P. Power [a,*]

[a] Department of Chemistry, University of California, Davis, CA 95616, United States
[b] Department of Chemistry, NanoScience Centre, University of Jyväskylä, P.O. Box 35, FI-40014 Jyväskylä, Finland
[c] Department of Chemistry, 2500 University Drive N.W., University of Calgary, Calgary, Alberta T2N 1N4, Canada

ARTICLE INFO

Dedicated to Peter T. Wolczanski in celebration of his 70th birthday

Keywords:
Main group
Thiolates
Dispersion energy
Organometallic

ABSTRACT

We report the isolation of a series of cyclohexyl-substituted, homoleptic main group arylthiolates, $\{Ge(SC_6H_2\text{-}2,4,6\text{-}Cy_3)_2\}_2$ (**1**), $\{Sn(SC_6H_2\text{-}2,4,6\text{-}Cy_3)_2\}_2$ (**2**), and $\{Pb(SC_6H_2\text{-}2,4,6\text{-}Cy_3)_2\}_2$ (**3**), as well as an improved one-pot synthesis of the thiol HSC_6H_2-2,4,6-Cy (**4**) with increased purity and yield. The solid-state structures of compounds **1**–**3** show that the group 14 atoms are bridged by two thiolato ligands whose hydrocarbon substituents are in either *cis* (**1** and **2**) or *trans* (**3**) conformations. In solution, the Ge(II) derivative **1** exists as a mixture of dimeric *cis* and *trans* isomers or as the monomer $Ge(SC_6H_2\text{-}2,4,6\text{-}Cy_3)_2$, as inferred from ^{1}H NMR data. Contrary to a previous report of derivatives of the isopropyl-substituted thiol HSC_6H_2-2,4,6-Pr^i_3, which led to the formation of a Ge(IV) hydride, no such hydride was observed during the synthesis of **1**. Computational studies showed that the dimeric structure of **1** is stabilized by intramolecular dispersion interactions that are higher than those in similar systems employing the isopropyl-substituted ligand, in agreement with the preferred formation of $HGe(SC_6H_2\text{-}2,4,6\text{-}Pr^i_3)_3$ over the putative dimer $\{Ge(SC_6H_2\text{-}2,4,6\text{-}Pr^i_3)_2\}_2$, although the exact mechanism leading to the hydride remains unclear. The corresponding Sn(II) derivative **2** is the first structurally characterized dimeric tin(II) thiolate. The Pb(II) species **3** is a rare example of a lead(II) arylthiolate that crystallizes in the absence of additional donor molecules.

1. Introduction

Despite well-established exchange reactions of the heavier group 14 silylamides [1,2] $M(N(SiMe_3)_2)_2$ (M = Ge, Sn, and Pb) with protic species to form a range of main group aryloxo compounds, [3–18] there are relatively few studies on low-coordinate (coordination number ≤ 3) Ge (II), Sn(II), and Pb(II) thiolates. The work of Lappert showed that the reactions of $M(N(SiMe_3)_2)_2$ with HSC_6H_3-2,6-Pr^i_2 (Pr^i = isopropyl) and HSC_6H_2-2,4,6-Bu^t_3 (Bu^t = *tert*-butyl) gave trimeric complexes $\{M(SC_6H_3\text{-}2,6\text{-}Pr^i_2)_2\}_3$ (M = Sn and Pb) as well as monomers $M(SC_6H_3\text{-}2,4,6\text{-}Bu^t_3)_2$ (M = Ge, Sn), and Pb.[19] Later studies also provided crystallographic data for Ge(II) arylthiolates, but the variety of characterized systems is limited to only a few anionic [20] and monomeric [21] species of the formula $[Ge(SC_6H_5)_3]^-$ and $Ge(SAr)_2$ (Ar = terphenyl-based ligand). In a similar fashion, X-ray crystallographic data on low-coordinate Sn(II) arylthiolates concern only some Sn(II) terphenyl complexes with the formula $Sn(SAr)_2$ (Ar = terphenyl-based ligand), [21] the structures reported by Lappert, [19] and two independent reports on the structure of the anion $[Sn(SC_6H_5)_3]^-$ with two different counter-cations. [22,23] In contrast, Pb(II) thiolates are notoriously difficult to crystallize in the absence of additional donors due to their tendency to polymerize, resulting in an inherent insolubility in hydrocarbon solvents. [24] Accordingly, only a few molecular Pb(II) arylthiolates free from Lewis-base stabilization have been structurally characterized in the solid state. Besides the work of Lappert, [19] these include species analogous to those of the lighter congeners, that is to say, the anion $[Pb(SC_6H_5)_3]^-$ [22,25,26] and the monomers $Pb(SAr)_2$ (Ar = terphenyl-based ligand),[17,21] as well as the dication $[Pb(SC_6H_4\text{-}4\text{-}NMe_3)_3]^{2+}$ and its trimeric analogue $[\{Pb(SC_6H_4\text{-}4\text{-}NMe_3)_2\}_3]^{6+}$ [27,28].

* Corresponding authors.
E-mail addresses: heikki.m.tuononen@jyu.fi (H.M. Tuononen), pppower@ucdavis.edu (P.P. Power).

https://doi.org/10.1016/j.poly.2024.116877
Received 7 November 2023; Accepted 31 January 2024
Available online 9 February 2024

In light of the existing structural data on low-coordinate Ge(II), Sn (II), and Pb(II) arylthiolates, we chose to try to isolate the first dimeric arylthiolate complexes of group 14 elements. To do this, a phenylthiol with cyclohexyl (Cy) substituents was chosen as they provide steric shielding [29,30] to an extent that lies roughly between that of isopropyl and *tert*-butyl groups that allowed the synthesis of the trimers {M(SC_6H_3-2,6-Pr^i_2)$_2$}$_3$ (M = Sn and Pb) and the monomers M(SC_6H_3-2,4,6-Bu^t_3)$_2$ (M = Ge, Sn, and Pb), respectively.[19] In addition, the three substituents Pr^i, Bu^t, and Cy have different dispersion energy donor properties, [31] with the bulky and spherical Bu^t substituents providing slightly stronger interactions than the smaller Pr^i and Cy groups. [32] We found that the use of cyclohexyl-substituted thiol led to the desired dimers {M(SC_6H_2-2,4,6-Cy_3)$_2$}$_2$ (M = Ge (**1**), Sn (**2**), and Pb (**3**)). These crystallize from their benzene or toluene solutions in good yield, thereby establishing the first structurally characterized series of homoleptic and dimeric M(II) arylthiolates. The detailed structural study of compounds **1**–**3** is augmented with a spectroscopic analysis of the behavior of the Ge (II) derivative **1** in solution, corroborated with computational investigations and a reactivity study of the new dimeric Sn(II) arylthiolate **2** with phenylacetylene and pinacolborane. Finally, the thiol used in the synthesis of **1**–**3**, HSC_6H_3-2,4,6-Cy_3 (**4**), has previously been employed as a hydrogen atom transfer catalyst, [33] but it has not been used as a ligand. An alternative synthetic method to **4** is reported herein that gives the thiol in excellent (80 %) yield and with high synthetic purity.

2. Results and discussion

2.1. Synthesis and structure of Ge(II) dimer

The reaction between two equivalents of the thiol HSC_6H_2-2,4,6-Cy_3 with one equivalent of Ge($N(SiMe_3)_2$)$_2$ gave the Ge(II) derivative {Ge(SC_6H_2-2,4,6-Cy_3)$_2$}$_2$ (**1**) as a monosolvate from benzene solution at room temperature. Its structure features C_2 symmetry and a *cis* arrangement of the arylthiolato ligands, with the cyclohexyl residues of the bridging ligands facing each other above and below the Ge_2S_2 core (Fig. 1). At 2.2753(8) Å, the Ge1–S1 bond distance is significantly shorter than the bridging Ge1–S2 and Ge1–S2A distances, 2.4105(8) and 2.5049(8) Å, respectively. However, at 1.802(3) and 1.798(3) Å, the S1–C1 and the S2– C25 distances involving the terminal and bridging ligands, respectively, are statistically identical. The Ge atom displays a distorted trigonal pyramidal geometry, with the sum of bond angles equaling 268.63(5)°. The C1–S1–Ge1 angle is 89.89(9)°, while the C25–S2–Ge1 angle involving the bridging ligand is significantly wider, 106.67(10)°.

Because no structures of dimeric Ge(II) arylthiolates have been reported to date, metrical comparisons of distances and angles were made with data for Ge(II) arylthiolate monomers [21,34] as well as for dimers with alkyl- [35] and silylthiolato [3] ligands (Table 1). The terminal Ge1–S1 distance in **1** is shorter than that in {Ge(SSi(Ph_3))$_2$}$^3_2$ but statistically identical with the average terminal Ge–S distance in {Ge(SBu^t)$_2$}$_2$ that carries a large standard uncertainty. [35] Interestingly, the terminal Ge1–S1 distance in **1** differs less than 0.2 Å from Ge–S distances in many monomeric Ge(II) arylthiolates with sterically encumbering terphenyl ligands, [21] with the short Ge–S bonds in the structure of Ge(SC_6H_3-2,6-(C_6H_2-2,4,6-Pr^i_3)$_2$)$_2$ making a noticeable exception. The bridging Ge1–S2 and Ge1–S2A distances in **1** differ by nearly 0.1 Å but their average value is similar to that in {Ge(SSi(Ph_3))$_2$}$_2$,[3] while longer than that in {Ge(SBu^t)$_2$}$_2$. [35] The S—C distances in **1** are shorter than those in alkyl-substituted dimers, [3,35] and much closer to those in monomeric Ge(II) arylthiolates with similar type of S—C bonds. [21] Compound **1** features the narrowest C—S—Ge angle of all related structurally characterized Ge(II) thiolates and contains the most puckered Ge_2S_2 core of all dimeric structures, [3,21,34,35] presumably owing to the spatial requirements of its sterically encumbering ligands in a *cis* arrangement.

Since we have previously investigated the importance of interligand H···H close (less than the sum of van der Waals radii of two hydrogen atoms, *ca.* 2.5 Å) [36] contacts to the stability of main group [37] and transition metal aryloxides, [38] a similar analysis was conducted for **1**. Interestingly, despite the favorable face-on orientation of the ligands, there are just five interligand H···H close contacts (≤2.5 Å) and this value remains unchanged if the threshold is increased to 2.6 Å (Fig. 2).

2.2. NMR spectroscopy and DFT calculations

The *in situ* room temperature ^{1}H NMR spectrum of **1** in C_6D_6 indicates that its solid-state structure is not retained in solution. Instead, a mixture of species is observed, which presumably contains *cis* and *trans* isomers of **1** and the monomer Ge(SC_6H_2-2,4,6-Cy_3)$_2$ (Equation 1), with the *cis* isomer being the preferred species.

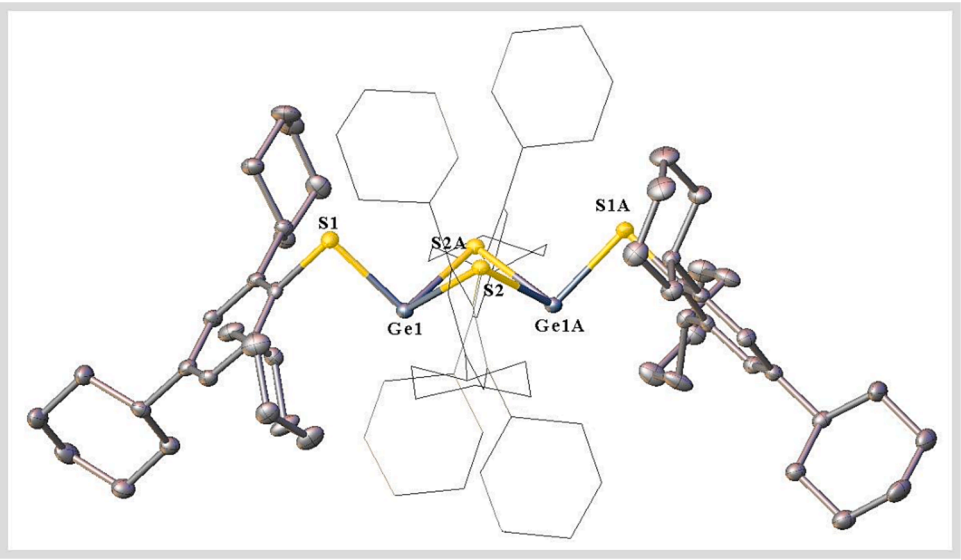

Fig. 1. Thermal ellipsoid (50 %) plot of {Ge(SC_6H_2-2,4,6-Cy_3)$_2$}$_2$ (**1**). Two ligands are shown wireframe format and all hydrogen atoms and the molecule of crystallization solvent (benzene) are not shown for clarity. Selected distances (Å) and angles (°): Ge1–S1 2.2753(8), Ge1–S2 2.4105(8), Ge1–S2A 2.5049(8), Ge1···Ge1A 3.26343(10), S1–C1 1.802(3), S2–C25 1.798(3), S1–Ge1–S2 98.27(3), S1–Ge1–S2A 97.98(3), S2–Ge1–S2A 72.38(3), C1–S1–Ge1 89.89(9), C25–S2–Ge1 106.67(10), C25–S2–Ge1A 121.65(10), Ge1–S2–Ge1A 83.17(3), $\Sigma_\angle$ Ge1 268.63(5).

Table 1
Selected Distances (Å) and Angles (°) for $\{Ge(SC_6H_2\text{-}2,4,6\text{-}Cy_3)_2\}_2$ (**1**) and in Related Ge(II) Thiolates.

Compound	Ge–S[b]	Ge–μS	C–S[b]–Ge	S[b]–Ge–S[c]	μS-Ge–μS	Ge–μS–Ge	S—C
$\{Ge(SC_6H_2\text{-}2,4,6\text{-}Cy_3)_2\}_2$ (**1**)	2.2753(8)	2.4105(8) 2.5049 (8)	89.89(9)	97.98(3) 98.27(3)	72.38(3)	83.17(3)	1.798(3) 1.802 (3)
$\{Ge(SBu^t)_2\}_2$ [35]	2.260(4)2.267 (4)	2.388(4)[a]2.465 (4)[a]	102.8(3)104.1 (3)	88.01(9)[a] 96.31 (9)[a]	85.37(5) 85.60 (9)	91.19(9) 91.46 (9)	1.855(4)[a]
$\{Ge(SSi(Ph_3))_2\}_2$ [3]	2.321(1)	2.472(1)2.4571 (9)	99.95(5)*	92.68(4) 94.12(4)	78.43(4)	88.43(3)	–
$Ge(SC(SiMe_3)_3)_2$ [34]	2.2272(6) 2.2274 (6)	–	108.44(6) 109.46 (7)	90.25(2)	–	–	1.865(2) 1.869 (2)
$Ge(SC_6H_3\text{-}2,6\text{-}(C_6H_2\text{-}2,6\text{-}Pr^i_2)_2)_2$ [21]	2.284(4)	–	113.58(5)	81.26(2)	–	–	1.778(1)
$Ge(SC_6H_3\text{-}2,6\text{-}(C_6H_2\text{-}2,4,6\text{-}Me_3)_2)_2$ [21]	2.2636(5) 2.2657 (6)	–	99.74(5)106.04 (6)	88.68(2)	–	–	1.784(2) 1.785 (2)
$Ge(SC_6H_3\text{-}2,6\text{-}(C_6H_2\text{-}2,4,6\text{-}Pr^i_3)_2)_2$ [21]	2.211(2)2.218 (3)	–	114.8(3)116.9 (3)	81.8(1)	–	–	1.756(8) 1.778 (8)
$Ge(SC_6H_1\text{-}2,6\text{-}(C_6H_2\text{-}2,4,6\text{-}Pr^i_3)_2\text{-}3,5\text{-}Pr^i_2)_2$ [21]	2.2940(6)	–	119.42(6)	77.01(2)	–	–	1.782(2)

[a] Average value. [b] Terminal S atom if dimeric structure. [c] Bridging S atom if dimeric structure. *Silicon atom in place of carbon.

For comparison, a singlet signal in the [29] Si spectrum of the dimer $\{Ge(SSi(Ph_3))_2\}_2$ indicated that it dissociates to $Ge(SSi(Y5Ph_3))_2$ monomers in $CDCl_3$ with no evidence of dynamic behavior at room temperature,[3] while the presence of both *cis* and *trans* isomers was reported for the related Ge(IV) species $(PhH_2C)(NR_2)Ge(\mu\text{-}S)_2Ge(NR_2)(CH_2Ph)$ (R = $SiMe_3$) in toluene.[39].

Initially, the presence of three separate signals in the aryl region of the ^{1}H NMR spectrum of a freshly prepared sample of **1** suggested that a Ge(IV) hydride $HGe(SC_6H_2\text{-}2,4,6\text{-}Cy_3)_3$, similar to that reported with the ligand $HSC_6H_2\text{-}2,4,6\text{-}Pr^i_3$,[18] may have formed. For $HGe(SC_6H_2\text{-}2,4,6\text{-}Pr^i_3)_3$, the hydride signal appears at 5.73 ppm and integrates to exactly 1H, with the remaining signals observed in the ^{1}H NMR spectrum being fully consistent with the structural characterization confirmed by X-ray crystallography.[18] In contrast, no signals were observed in the ^{1}H NMR spectrum of **1** around 5.7 ppm and the signals observed in the aryl region could not be rationalized by assuming a single species, namely the hydride $HGe(SC_6H_2\text{-}2,4,6\text{-}Cy_3)_3$. Consequently, a second sample of **1** was synthesized, crystallized, and structurally characterized by X-ray diffraction. The ^{1}H NMR spectrum of the new sample matched that of the original, with three separate signals in the aryl region. To assign these signals, the reaction between $Ge(N(SiMe_3)_2)_2$ and $HSC_6H_2\text{-}2,4,6\text{-}Cy_3$ was monitored *via* ^{1}H NMR spectroscopy to reference the observed signals to the $HN(SiMe_3)_2$ formed in the reaction, thereby allowing the determination of which of the aryl signals observed was the residual solvent signal of C_6D_6. Setting the methine signal at 3.67 ppm to exactly 4H, followed by integration of the remaining signals, gave a good match with the dimeric structure of *cis* **1** for all but three key signals in the spectrum. Two of these reside in the aryl region, at 6.97 and 6.12 ppm, integrating to *ca.* 1.50 and 1.30H, respectively, while the third one involves the entire cyclohexyl methylene region spanning from 1.20 to 2.03 ppm and integrating to 162H. Provided the reaction yields no side products, such as the hydride $HGe(SC_6H_2\text{-}2,4,6\text{-}Cy_3)_3$, the integration of the methyl signal for $HN(SiMe_3)_2$ at 0.09 ppm should afford 72 hydrogens, following the employed stoichiometry (Eq 1). Setting the key methyl signal to exactly 72 H led to the same integration ratios observed earlier, which could be explained by assuming the presence of both *cis* and *trans* isomers of **1**. The original assumption was that the signal at 6.12 ppm corresponds to the monomeric germylene. However, a VT-study of a dilute, crystalline sample of **1** revealed that the signal at 6.12 ppm was no longer present, and that this peak in the *in situ* spectrum indicates the formation of an unidentifiable intermediate that is in equilibrium with the desired dimeric species **1**. Instead, the spectrum of the dilute sample of **1** showed a single aryl resonance at 7.20 ppm that did not change in intensity as a function of temperature and is thereby assigned to the monomeric germylene. These data suggest that at low concentrations, the structure of **1** is monomeric, while a dimeric structure is favored in saturated solutions.

To further investigate the different isomers of **1** and the monomeric germylene (Scheme 1), all three species in question were examined computationally with density functional theory (DFT) using a universal solution model (SMD). The results (Fig. 3) show that the dimerization of the germylene monomer $Ge(SC_6H_2\text{-}2,4,6\text{-}Cy_3)_2$ is favored by 43 kJ mol^{-1}, while the *cis* isomer of **1** is energetically comparable with the *trans* isomer. Thus, provided that the *cis–trans* isomerization has a sizable kinetic barrier owing to the bulky substituents, while that associated with the exchange of bridging and terminal ligands is smaller, the calculations provide support for the coexistence of the *cis* and *trans* isomers of **1** in solution. Furthermore, as implied by the calculated energies excluding empirical dispersion correction (Fig. 3), the dimerization is greatly driven by dispersion energy stabilization, whose effect is most likely overestimated as the calculations do not consider ligand dynamics (rotation of substituents) in solution. Even though the *cis* isomer of **1** is certainly the preferred species in the solid state, the monomer–dimer balance is less clear in solution. Complex **1** can dissociate to monomers at low concentrations provided that the associated energy barrier is of appropriate height.

As discussed above, a reaction between $Ge(N(SiMe_3)_2)_2$ and $HSC_6H_2\text{-}2,4,6\text{-}Pr^i_3$ has been reported to yield the Ge(IV) hydride $HGe(C_6H_2\text{-}2,4,6\text{-}Pr^i_3)_3$ irrespective of stoichiometry (1:2 or 1:3), with no indication of the formation of the dimer $\{Ge(SC_6H_2\text{-}2,4,6\text{-}Pr^i_3)_2\}_2$ or the monomer $Ge(SC_6H_2\text{-}2,4,6\text{-}Pr^i_3)_2$. [18] In contrast, a reaction between $Ge(N(SiMe_3)_2)_2$ and the selenol $HSeC_6H_2\text{-}2,4,6\text{-}Me_3$ is known to form the tetra-substituted Ge(IV) species $Ge(SeC_6H_2\text{-}2,4,6\text{-}Me_3)_4$.[40] The formation $Ge(SeC_6H_2\text{-}2,4,6\text{-}Me_3)_4$ was monitored *via* ^{1}H NMR and ^{77}Se NMR spectroscopy and two intermediates were detected along with the formation of H_2 gas. The first intermediate was identified as the germylene $Ge(SeMes)_2$, which reacts with another equivalent of the selenol to form a Ge(IV) hydride $HGe(SeC_6H_2\text{-}2,4,6\text{-}Me_3)_3$ and, ultimately, $Ge(SeC_6H_2\text{-}2,4,6\text{-}Me_3)_4$.[40] We therefore calculated the energies associated with the formation of the Ge(IV) hydride and compared the results obtained for the two related ligands $–SC_6H_2\text{-}2,4,6\text{-}Cy_3$ and $–SC_6H_2\text{-}2,4,6\text{-}Pr^i_3$. As shown in Fig. 3, the dimerization of $Ge(SC_6H_2\text{-}2,4,6\text{-}Pr^i_3)_2$ is favored only by 17 kJ mol^{-1} in solution (*cf.* 43 kJ mol^{-1} for $Ge(SC_6H_2\text{-}2,4,6\text{-}Cy_3)_2$), with a significantly smaller dispersion component compared to its cyclohexyl analogue. As ligand dynamics are not accounted for, the stability of the Ge(IV) hydrides in solution is likely slightly

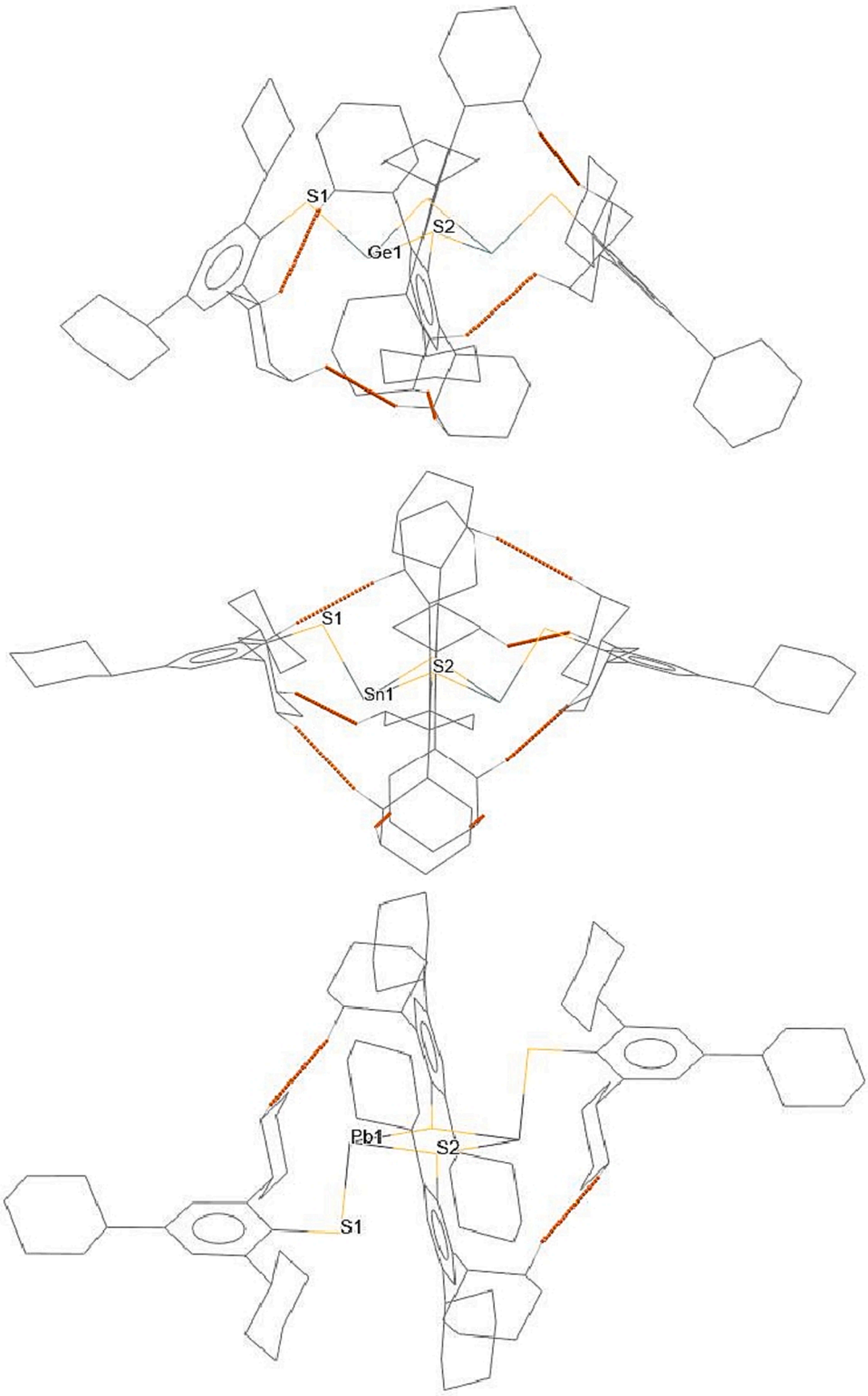

Fig. 2. Wireframe structures of **1** (top), **2** (middle), and **3** (bottom) illustrating the location of close (≤2.5 Å) interligand H···H contacts (orange dashed lines) from two orientations. Crystallization solvents (benzene and toluene) and hydrogen atoms not involved in the visualized H···H contacts are not shown for clarity.

$$2\ Ge(N(SiMe_3)_2)_2 + 4\ HSC_6H_2\text{-}2,4,6\text{-}Cy_3 \rightarrow\ x\ cis\text{-}\{Ge(SC_6H_2\text{-}2,4,6\text{-}Cy_3)_2\}_2 + y\ trans\text{-}\{Ge(SC_6H_2\text{-}2,4,6\text{-}Cy_3)_2\}_2 + z\ Ge(SC_6H_2\text{-}2,4,6\text{-}Cy_3)_2 + 4\ HN(SiMe_3)_2$$

Scheme 1. Proposed equilibrium between the monomeric germylene and the isomers of **1** in saturated solution.

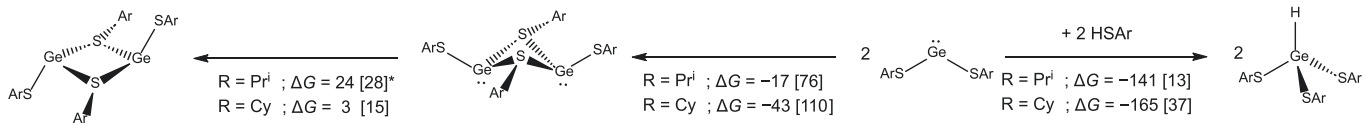

Fig. 3. Calculated Gibbs energies (benzene, 298.15 K, kJ mol^{-1}) of reactions involving dimerization of monomeric Ge(II) arylthiolates Ge(SAr)$_2$ (Ar = -C$_6$H$_2$-2,4,6-R_3) and their oxidative addition with the arythiol HSAr. Values in square brackets exclude empirical dispersion correction. * The C_i-symmetric *trans* isomer of {Ge(SC$_6$H$_2$-2,4,6-Pr$^i_3$)$_2$}$_2$ has one imaginary frequency leading to puckering of the Ge$_2$S$_2$ ring.

overestimated. Irrespective of this, the hydrides are clearly the thermodynamically most favored products regardless of the identity of the substituent on the aryl ligand (Pr^i or Cy). In the publication reporting the synthesis of HGe(SC$_6$H$_2$-2,4,6-Pr$^i_3$)$_3$, the formation of a Ge(IV) hydride over other possible products was rationalized by assuming that the rate of insertion of the Ge(II) atom to the H—S bond in the thiol is faster than the rate of proton transfer from the thiol to the amide.[18] Our calculations show that the transition state for the insertion of Ge(SC$_6$H$_2$-2,4,6-Pr$^i_3$)$_2$ or Ge(SC$_6$H$_2$-2,4,6-Cy$_3$)$_2$ to the H—S bond in HSC$_6$H$_2$-2,4,6-Pr$^i_3$ or HSC$_6$H$_2$-2,4,6-Cy$_3$, respectively, has a Gibbs energy of activation of *ca.* 120 kJ mol^{-1} irrespective of the substituent, which disagrees with the experimental reaction rate indicating completion within minutes. Hence, taking all the above into account, the results from DFT calculations support the notion that dispersion interactions play a greater role in cyclohexyl-substituted Ge(II) arylthiolates over the corresponding isopropyl-substituted derivatives, rendering the formation of the dimer {Ge(SC$_6$H$_2$-2,4,6-Pr$^i_3$)$_2$}$_2$ less probable than that of **1**, both in solution and in the solid state, as observed experimentally. Furthermore, even though the Ge(IV) hydrides HGe(SC$_6$H$_2$-2,4,6-Pr$^i_3$)$_3$ and HGe(SC$_6$H$_2$-2,4,6-Cy$_3$)$_3$ are calculated to be thermodynamically the most favored products in solution, they are unlikely to form through the addition of a Ge(II) monomer to the H—S bond in the corresponding arylthiol, as suggested earlier.[18] At this point, the mechanism for the formation of HGe(SC$_6$H$_2$-2,4,6-Pr$^i_3$)$_3$ is unclear but it must involve a process that is unattainable for the heavier cyclohexyl ligand HSC$_6$H$_2$-2,4,6-Cy$_3$ because HGe(SC$_6$H$_2$-2,4,6-Cy$_3$)$_3$ was not observed in our experiments.

2.3. Synthesis and structures of Sn(II) and Pb(II) dimers

The Sn(II) derivative {Sn(SC$_6$H$_2$-2,4,6-Cy$_3$)$_2$}$_2$ (**2**) is the first dimeric Sn(II) arylthiolate. It was synthesized in an analogous manner to **1** and crystallizes readily as large, colorless blocks from benzene solution. Unlike **1**, the *in situ* room temperature ^{1}H NMR spectrum of **2** in C$_6$D$_6$ shows a single signal in the aryl region, suggesting the presence of only one species. However, all signals in the ^{1}H NMR spectrum are broadened, indicating a dynamic process that equalizes the signals of the bridging and terminal ligands. Unfortunately, no ^{119}Sn NMR signal was detected at room temperature and variable temperature NMR studies were not performed.

Compound **2** crystallizes from benzene as a disolvate (Fig. 4). Like its germanium analogue **1**, the solid-state structure of **2** features C_2 symmetry and a *cis* arrangement of the arylthiolato ligands. Even though the synthesis of a dimeric Sn(II) silylthiolate {Sn(SSi(SiMe$_3$)$_3$)$_2$}$_2$ has been reported,[41] no crystallographic data are available for it, precluding structural comparisons. Consequently, compounds that are most closely related to **2** include the trimer {Sn(SC$_6$H$_3$-2,6-Pr^i)$_2$}$_3$ [19] and a series of Sn(II) arylthiolate monomers (Table 2).[19,21] At 2.4567(7) Å, the Sn1–S1 distance in **2** is comparable to the terminal Sn–S distance in the trimer {Sn(SC$_6$H$_3$-2,6-Pr^i)$_2$}$_3$, 2.471(5) Å. The same also holds between **2** and many Sn(II) arylthiolate monomers, though the Sn–S distance in the derivative Sn(SC$_6$H$_2$-2,4,6-Bu$^t_3$)$_2$ is particularly short, 2.4356(3), [19] while that in Sn(SC$_6$H$_1$-2,6-(C$_6$H$_2$-2,4,6-Pr$^i_3$)$_2$–3,5-Pr$^i_2$)$_2$ with eight isopropyl substituents on each ligand is noticeably long, 2.5009(6) Å. [21] The Sn1–S2 and Sn1–S2A bonds in **2** differ by less than 0.02 Å and are, rather expectedly, longer than the terminal Sn1–S1 bond in **2** and the related Sn–S distances in the trimer {Sn(SC$_6$H$_3$-2,6-Pr^i)$_2$}$_3$.[19] The C1–S1–Sn1 angle in **2** is narrower than the corresponding angle in most structurally characterized Sn(II) arylthiolates, though wider than that in the trimer {Sn(SC$_6$H$_3$-2,6-Pr^i)$_2$}$_3$;[19] the C1–S1–Sn1 angle is also significantly less acute than the C1–S1–Ge1 angle in **1**. The S2–Sn1–S2A angle in **2** is very acute, 66.46(2)°, but the only available reference value, 74.4(1)°, is from a trimeric structure and, therefore, not strictly comparable. [19] A comparison of the sum of bond angles for the group 14 element in **1** and **2** shows a *ca.* 20° decrease on moving from Ge(II) to Sn(II), illustrating that the M$_2$S$_2$ core (M = Ge, Sn) is more puckered in **2** than in **1**. Compound **2** features eight interligand H···H close contacts

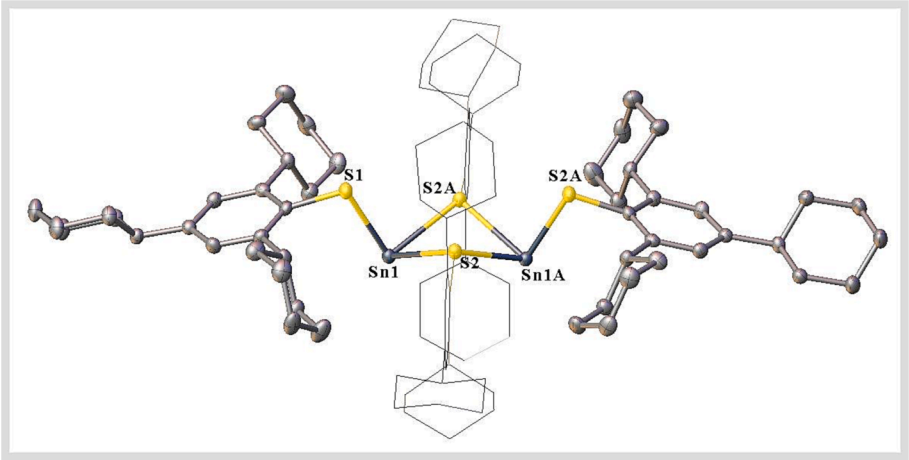

Fig. 4. Thermal ellipsoid (50 %) plot of {Sn(SC$_6$H$_2$-2,4,6-Cy$_3$)$_2$}$_2$ (**2**). Two ligands are shown in wireframe format and all hydrogen atoms and co-crystallized solvent molecules (benzene) are not shown for clarity. Atoms C43–C48 and Sn1 are disordered over two positions, with only the higher occupancy (92 % and 98 %, respectively) atoms shown. Selected distances (Å) and angles (°): Sn1–S1 2.4567(7), Sn1–S2 2.6235(6), Sn1–S2A 2.6390(6), Sn1···Sn1A 3.8710(11), S1–C1 1.799(2), S2–C25 1.783(2), S1–Sn1–S2 90.58(2), S1–Sn1–S2A 91.66(2), S2–Sn1–S2A 66.46(2), C1–S1–Sn1 100.35(8), C25–S2–Sn1 116.36(8), C25–S2–Sn1A 120.08(8), Sn1–S2–Sn1A 94.70(2), $\Sigma_\angle$ Sn1 248.70(3).

Table 2
Selected Distances (Å) and Angles (°) for $\{Sn(SC_6H_2\text{-}2,4,6\text{-}Cy_3)_2\}_2$ (**2**) and Related Sn(II) Thiolates.

Compound	Sn–S[b]	Sn–μS	C–S[b]–Sn	S[b]–Sn–S[c]	μS–Sn–μS	Sn–μS–Sn	S—C
$\{Sn(SC_6H_2\text{-}2,4,6\text{-}Cy_3)_2\}_2$ (**2**)	2.4567(7)	2.6235(6)2.6391 (6)	100.35(8)	90.58(2) 91.66 (2)	66.46(2)	94.70(2)	1.783(2)1.799 (2)
$\{Sn(SC_6H_3\text{-}2,6\text{-}Pr^i)_2\}_3$ [19]	2.471(5)	2.583(3) 2.6428 (4)	96.829(8)	89.8(2)95.0 (1)	74.4(1)	96.758(13) 101.662 (12)	1.8146(3)[a]
$Sn(SC_6H_2\text{-}2,4,6\text{-}Bu^t_3)_2$ [19]	2.4356(3)	–	101.64(12)	85.4(1)	–	–	1.8087(2)
$Sn(SC_6H_3\text{-}2,6\text{-}(C_6H_2\text{-}2,6\text{-}Pr^i_2)_2)_2$ [21]	2.470(1)	–	113.8(1)	78.63(3)	–	–	1.778(4)
$Sn(SC_6H_3\text{-}2,6\text{-}(C_6H_2\text{-}2,4,6\text{-}Me_3)_2)_2$ [21]	2.4744(4)2.4844 (4)	–	98.88(4)108.61 (4)	85.55(1)	–	–	1.781(1)1.782 (1)
$Sn(SC_6H_3\text{-}2,6\text{-}(C_6H_2\text{-}2,4,6\text{-}Pr^i_3)_2)_2$ [21]	2.4723 (5)[§]2.4813 (4)[§]	–	111.55 (5)[§]113.69 (6)[§]	78.27(2)[§]	–	–	1.776 (2)[§]1.777 (2)[§]
$Sn(SC_6H_1\text{-}2,6\text{-}(C_6H_2\text{-}2,4,6\text{-}Pr^i_3)_2\text{-}3,5\text{-}Pr^i_2)_2$ [21]	2.5009(6)	–	119.15(8)	73.09(2)	–	–	1.776(2)

[a] Average value. [b] Terminal S atom if dimeric/trimeric [c.] Bridging S atom if dimeric or trimeric structure. [§] Data is reported for only one crystallographically identical molecule.

Table 3
Selected Distances (Å) and Angles (°) for $\{Pb(SC_6H_2\text{-}2,4,6\text{-}Cy_3)_2\}_2$ (**3**) and Related Pb(II) Thiolates.

Compound	Pb–S[b]	Pb–μS	C–S[b]–Pb	S[b]–Pb–S[c]	μS–Pb–μS	Pb–μS–Pb	S—C
$\{Pb(SC_6H_2\text{-}2,4,6\text{-}Cy_3)_2\}_2$ (**3**)	2.5522(5)	2.722(11)[a]	93.29(6)	89.542(16)99.244 (15)	71.138 (15)	108.863 (15)	1.7828(18) 1.7890 (19)
$\{Pb(SSi(OBu^t)_3)_2\}_2$ [42]	2.585(5)[a]	2.768(3)[a] 2.808 (4)[a]	98.7(7)[a]*	88.7(9)[a] 93.1(8)[a]	79.2(6)[a]	90.0(2)[a]	–
$\{Pb(SC_6H_3\text{-}2,6\text{-}Pr^i)_2\}_3$ [19]	2.5534(9)	2.6738(8) 2.7806 (3)	98.035(12)	92.64(9)92.77 (9)	73.493 (19)	–	1.7586(4)[a]
$Pb(SC_6H_3\text{-}2,6\text{-}(C_6H_3\text{-}2,6\text{-}Pr^i_2)_2)_2$ [17]	2.56(9)	–	113.42(11)	77.21(4)	–	–	1.771(3)
$Pb(SC_6H_3\text{-}2,6\text{-}(C_6H_3\text{-}2,4,6\text{-}Pr^i_3)_2)_2$ [21]	2.5746(6) 2.5838 (6)	–	114.16(6) 115.63 (5)	77.27(2)	–	–	1.770(2)1.773 (2)
$Pb(SC_6H_1\text{-}2,6\text{-}(C_6H_2\text{-}2,4,6\text{-}Pr^i_3)_2\text{-}3,5\text{-}Pr^i_2)_2$ [21]	2.5797(7) 2.5940 (5)	–	116.49(5) 118.35 (5)	80.07(2)	–	–	1.781(2)1.783 (1)

[a] Average value. [b] Terminal S atom if dimeric/trimeric [c] Bridging S atom if dimeric or trimeric structure. * Silicon atom in place of carbon.

(≤2.5 Å) (Fig. 2), suggesting that the role of dispersion interactions in stabilizing its solid-state structure might be even greater than that for **1** (Table 3).

The hydrophobic character of the cyclohexane substituents gave the Pb(II) derivative $\{Pb(SC_6H_2\text{-}2,4,6\text{-}Cy_3)_2\}_2$ (**3**) sufficient solubility in hexane, benzene, and toluene to allow its isolation and crystallization in the absence of additional Lewis bases. Like its aryloxo analogue $\{Pb(OC_6H_2\text{-}2,4,6\text{-}Cy_3)_2\}_2$ and other related Pb(II) chalcogenolates,[37] **3** is thermochromic and turns red above *ca.* 80 °C in toluene and returns to orange at room temperature. Moreover, compound **3** is stable in the

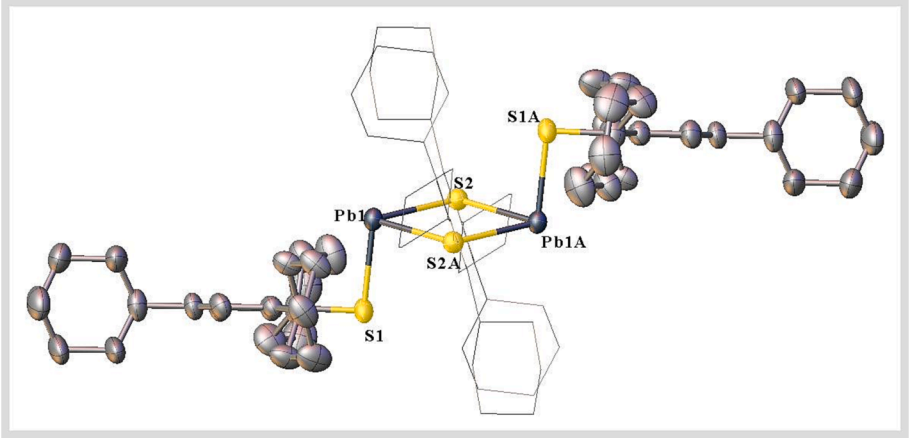

Fig. 5. Thermal ellipsoid (50 %) plot of $\{Pb(SC_6H_2\text{-}2,4,6\text{-}Cy_3)_2\}_2$ (**3**). Ligands are shown in wireframe format and all hydrogen atoms and co-crystallized solvent molecules (toluene) are not shown for clarity. Atoms C43–C48 and C19–C24 are disordered over two positions, with only the higher occupancy (65 %) atoms shown. Selected distances (Å) and angles (°): Pb1–S1 2.5522(5), Pb1–S2 2.7138(5), Pb1–S2A 2.7294(5), Pb···Pb 4.4276(9), S1–C1 1.7890(19), S2–C25 1.7828(18), S1–Pb1–S2 99.244(15), S1–Pb1–S2A 89.542(16), S2–Pb1–S2A 71.138(15), C1–S1–Pb1 93.29(6), C25–S2–Pb1 117.65(6), C25–S2–Pb1A 121.89(6), Pb1–S2–Pb1A 108.863(15), $\Sigma_\angle$ Pb1 259.924(27).

presence of light both in solution and in the solid state. The *in situ* room temperature ^{1}H NMR spectrum of **3** in C_6D_6 shows two resonances in the aryl region with broadening of signals, indicating of a mixture of species and/or a dynamic process in solution. Unfortunately, no ^{207}Pb NMR signal was detected at room temperature and variable temperature NMR studies were not performed.

In contrast to the solid-state structures of **1** and **2**, **3** displays C_i symmetry and a *trans* arrangement of ligands similar to that observed in $\{Pb(OC_6H_2\text{-}2,4,6\text{-}Cy_3)_2\}_2$ (Fig. 5).[37] The Pb1–S1 bond in **3** is shorter than the related Pb–S bond in the other reported dimeric Pb(II) thiolate, [42] but comparable to that in the trimer $\{Pb(SC_6H_3\text{-}2,6\text{-}Pr^i_2)_2\}_3$.[19] The C1–S1–Pb1 angle in **3** is significantly more acute than the related angles in other Pb(II) alkyl- or arylthiolates, presumably owing to the *trans* orientation of the terminal ligands in **3**, which also rationalizes the *ca.* 10° difference between the S1–Pb1–S2 and S1–Pb1–S2A angles. Consequently, the metrical parameters of the Pb_2S_2 core in **3** are not strictly comparable to those in the other dimeric Pb(II) thiolate since the Pb_2S_2 ring is planar in **3** but it is puckered in $\{Pb(SSi(OBu^t)_3)_2\}_2$.[42] The *trans* arrangement of substituents in **3** also affects the S2–Pb1–S2A and Pb1–S2–Pb1A angles, making the former narrower and the latter wider compared to the corresponding angles in the dimer $Pb(SSi(OBu^t)_3)_2\}_2$.[42] Compound **3** has only two interligand H···H close contacts (≤2.5 Å) (Fig. 2) compared to the eight interactions present in its aryloxo analogue $\{Pb(OC_6H_2\text{-}2,4,6\text{-}Cy_3)_2\}_2$ with significantly shorter Pb–O bonds compared to the Pb–S distances in **3**.[37] The value of interligand H···H close contacts increases to four if the threshold is increased to 2.6 Å. This suggests that the role of dispersion interactions in stabilizing the dimeric solid-state structure of **3** should be the smallest of the three compounds considered.

3. Reactivity studies

Considering that **2** crystallizes readily in high yield and its synthesis involves relatively inexpensive starting materials, reactivity studies with selected molecular substrates were conducted in an attempt to isolate new, monomeric Sn(II) species. Addition of two equivalents of pinacolborane to one equivalent of **2** at *ca.* −18 °C in hexane led to immediate color change and precipitation of a tan powder that could not be identified by ^{1}H NMR spectroscopy. This insoluble tan powder likely originates from the dismutation of pinacolborane.[43,44] Filtration of the dark orange solution, followed by its concentration and storage at *ca.* −18 °C led to the precipitation of colorless crystals after 48 h. X-ray crystallography and ^{1}H NMR spectroscopy confirmed that the crystals are unambiguously **2**. Filtration of the supernatant liquid from the crystalline material followed by further concentration produced a second crop of colorless crystals of **2** and repeated fractional crystallizations provided no other identifiable products. In a similar fashion, addition of two equivalents of phenylacetylene to one equivalent of **2** in benzene and refluxing the solution for 4 days in a J. Young ampoule produced a large cluster of colorless crystals when the solution was cooled to room temperature. Analysis by X-ray crystallography and ^{1}H NMR spectroscopy confirmed the crystalline material to be pure **2** that could be recovered in 99 % yield by mass analysis.

3.1. Ligand synthesis

While a synthesis of $HSC_6H_2\text{-}2,4,6\text{-}Cy_3$ (**4**) has been published, [33,45] contaminants were clearly present in the published spectroscopic data despite purification by column chromatography (SiO_2, pentane).[33] An improved one-pot synthesis of the thiol **4** was undertaken using *in situ* lithiation of $BrC_6H_2\text{-}2,4,6\text{-}Cy_3$[45] with *t*-butyl lithium. This afforded the thiol in good yield and excellent purity, with no extraneous signals present in the NMR spectra. Furthermore, purification *via* column chromatography was not required after the organic work-up since **4** can be crystallized in large quantity from a concentrated, boiling ethyl acetate solution. After isolation of the first crop of crystals, a second crop could be collected from the mother liquor after *ca.* 2 days *via* slow evaporation of the solvent to give an overall yield of *ca.* 80 %. While all spectroscopic data obtained for **4** matches those reported previously,[33] an X-ray crystallographic determination of its structure (Fig. S12) was not presented.

4. Conclusions

We have synthesized and characterized three new arylthiolato complexes of group 14 elements M(II) (M = Ge, Sn, and Pb). The compounds $\{Ge(SC_6H_2\text{-}2,4,6\text{-}Cy_3)_2\}_2$ (**1**), $\{Sn(SC_6H_2\text{-}2,4,6\text{-}Cy_3)_2\}_2$ (**2**), and $\{Pb(SC_6H_2\text{-}2,4,6\text{-}Cy_3)_2\}_2$ (**3**) all have dimeric structures in the solid state, with **1** and **2** showing a *cis* arrangement of ligands while **3** displays a *trans* orientation. Collectively, **1**–**3** establish a unique crystallographically characterized series of dimeric group 14 arylthiolates. Specifically, **2** is the first dimeric Sn(II) thiolate with structural data available, while **3** is a rare example of a Pb(II) thiolate that crystallizes in the absence of additional donor ligands. The sterically encumbering ligand $–SC_6H_2\text{-}2,4,6\text{-}Cy_3$, used for the first time for the synthesis of metal complexes, gives compounds **1**–**3** structural features that differentiate them from related systems reported in the literature. In contrast to the dimeric structures observed in the solid state, NMR studies of **1**–**3** indicated the presence of a dynamic process in solution at room temperature, which in the case of the Ge(II) derivative leads to a mixture of species, presumably containing the *cis* and *trans* isomers of **1** and the monomeric germylene $Ge(SC_6H_2\text{-}2,4,6\text{-}Cy_3)_2$. Results from computational studies indicated that the *cis* isomer of **1** is the energetically preferred species in solution, largely owing to the significant stabilization provided by intramolecular dispersion, though the *trans* isomer is energetically comparable and the dissociation of **1** to the corresponding monomers is a plausible explanation for the species observed in the ^{1}H NMR spectra recorded from a dilute solution of **1**. The calculations also demonstrated that the addition of $Ge(SC_6H_2\text{-}2,4,6\text{-}Pr^i_3)_2$ to the H—S bond in $HSC_6H_2\text{-}2,4,6\text{-}Pr^i_3$ is associated with a high energy barrier and is therefore a less-likely route to the Ge(IV) hydride $HGe(SC_6H_2\text{-}2,4,6\text{-}Pr^i_3)_3$ reported earlier. This result agrees with the fact that its cyclohexyl analogue $HGe(SC_6H_2\text{-}2,4,6\text{-}Cy)_3$ was not observed in any of the performed experiments, even though the Ge(IV) hydride was calculated to be the thermodynamic sink on the potential energy surface. Reactions of Sn(II) arylthiolate **2** with pinacolborane and phenylacetylene yielded only crystalline starting material despite the use of forceful conditions, which implies of the thermodynamic stability of the dimeric structure of **2** in the solid state. Finally, a one-pot synthetic procedure was devised for the thiol $HSC_6H_2\text{-}2,4,6\text{-}Cy_3$ (**4**), giving it in high (*ca.* 80 %) yield and with excellent synthetic purity.

5. Experimental section

5.1. General considerations

All manipulations were carried out under anaerobic and anhydrous conditions by using standard Schlenk techniques or in a Vacuum Atmospheres OMNI-Lab drybox under an atmosphere of dry argon or nitrogen. Solvents were dried by the method of Grubbs and co-workers, [46] stored over potassium or sodium, and then degassed by the freeze–pump–thaw method. All physical measurements were made under strictly anaerobic and anhydrous conditions. Melting points of samples were determined in flame-sealed capillaries using a Meltemp II apparatus equipped with a partial immersion thermometer with a device limit of 250 °C. IR spectra were recorded as Nujol mulls between CsI plates on a PerkinElmer 1430 spectrometer. UV–Vis spectra were recorded as dilute toluene solutions in 3.5 mL quartz cuvettes using a modernized Olis 17 Cary 14 UV–Vis–Near-IR spectrophotometer. NMR spectra were recorded on a Varian Inova 600 MHz spectrometer or a Bruker 400 MHz AVANCE III HD Nanobay spectrometer, and the ^{1}H NMR spectra were referenced to the residual solvent signals in

deuterated benzene (**1**–**3**) or deuterated chloroform (**4**). Unless otherwise stated, all materials were obtained from commercial sources and used as received. The ligand 2,4,6-tricyclohexylphenylthiol was synthesized based on a modified literature procedure.[33] Group 14 silylamides $M(N(SiMe_3)_2)_2$ (M = Ge, Sn, and Pb) were synthesized by published procedures.[1,2] Compounds **1**–**3** were synthesized *via* protonolysis between one equivalent of $M(N(SiMe_3)_2)_2$ (M = Ge, Sn, and Pb) and two equivalents of HSC_6H_2-2,4,6-Cy_3 (Cy = cyclohexyl) in *ca.* 80 mL of hexanes at room temperature. The solutions were stirred for 2 h after which the solvent was exchanged for benzene or toluene (*vide infra*).

5.2. X-ray crystallographic studies

Crystals of **1**–**3** suitable for X-ray crystallographic studies were obtained from saturated benzene (**1** and **2**) and toluene (**3**) solutions upon standing for 24 h at room temperature. The crystals were removed from the Schlenk tubes and immediately covered with a layer of hydrocarbon oil. Suitable crystals were selected, mounted on a nylon cryoloop, and then placed in the cold nitrogen stream of the diffractometer. Data for **1**, **2**, and **3** were collected at 90(2) K with Mo $K\alpha_1$ radiation ($\lambda = 0.71073$ Å) using a Bruker D8 Venture dual source diffractometer in conjunction with a CCD detector. The collected reflections were corrected for Lorentz and polarization effects and for absorption by using Blessing's method as incorporated into the program SADABS.[47,48] The structures were solved by direct methods and refined with the SHELXTL (2012, version 6.1) or SHELXTL (2013) software packages.[49] Refinement was by full-matrix least-squares procedures, with all carbon-bound hydrogen atoms included in calculated positions and treated as riding atoms. The thermal ellipsoid plots were drawn using OLEX2 software.[50].

5.3. Synthesis

$\{Ge(SC_6H_2$-2,4,6-$Cy_3)_2\}_2$ (**1**). 0.657 g (1.843 mmol) of HSC_6H_2-2,4,6-Cy_3 and 0.362 g (0.921 mmol) of $Ge(N(SiMe_3)_2)_2$ were combined in a 100 mL Schlenk flask and dissolved in hexane to give a yellow solution. The flask was dried at *ca.* 40 °C under reduced pressure (*ca.* 0.01 torr) and the solvent was exchanged for benzene. Room temperature crystallization from *ca.* 20 mL benzene solution gave 0.383 g (53.1 %) of **1** as colorless crystalline material. X-ray quality single crystals were obtained from hot (*ca.* 80 °C) benzene-d_6 solution in a J. Young NMR tube.

^{1}H NMR (400 MHz, C_6D_6, 25 °C, δ/ppm, *in situ*, saturated sample): 7.14 (8H, *cis*), 6.97 (1.17H, *trans*), 6.12 (1.25H, *intermediate*), 3.67 (4H), 2.48 (8H), 2.03–1.20 (162H), 0.09 (72H, *H*N(SiMe$_3$)$_2$). IR (Nujol, $\tilde{\nu}$/cm^{-1}): 2960 (s), 2925 (s), 2860 (s), 2600 (w), 1600 (w), 1560 (w), 1450 (m, broad), 1350 (w, broad), 1260 (s), 1100 (s), 1020 (s), 930 (w), 800 (s), 680 (m), 620 (w), 560 (w), 530 (w), 500 (w), 430 (w), 395 (w), 370 (w), 290 (w). UV–vis (λ/nm; ε/M^{-1} cm^{-1}): 283 (3,300). ^{1}H NMR (400 MHz, C_6D_6, 25 °C, δ/ppm, dilute, crystalline sample): 7.20 (4H), 3.62 (4H), 2.50 (2H), 1.94–1.30 (*cyclohexyl*) Melting point: > 250 °C.

$\{Sn(SC_6H_2$-2,4,6-$Cy_3)_2\}_2$ (**2**). 0.961 g (2.695 mmol) of HSC_6H_2-2,4,6-Cy_3 and 0.592 g (1.347 mmol) of $Sn(N(SiMe_3)_2)_2$ were combined in a 100 mL Schlenk flask and dissolved in hexane to give a light-yellow solution. The flask was dried at *ca.* 40 °C under reduced pressure (*ca.* 0.01 torr) and the solvent was exchanged for benzene. Crystallization from slowly cooling a *ca.* 30 mL hot (*ca.* 80 °C) benzene solution gave 0.686 g (61.4 %) of **2** as colorless X-ray quality single crystals.

^{1}H NMR (400 MHz, C_6D_6, 25 °C, δ/ppm): 7.14–7.11 (8H), 3.89 (6H), 2.44 (6H), 1.94–1.12 (120H). IR (Nujol, $\tilde{\nu}$/cm^{-1}): 2925 (s), 2860 (s), 2670 (w), 1600 (m), 1560 (m), 1450 (m), 1380 (m), 1350 (m), 1270 (m), 1240 (w), 1170 (w), 1100 (m), 1060 (m), 1025 (m), 1000 (w), 950 (w), 890 (w), 870 (m), 850 (w), 810 (m), 755 (w), 730 (w), 680 (w), 630 (w), 535 (w), 435 (w), 320 (w), 270 (w). UV–vis (λ/nm; ε/M^{-1}cm^{-1}): 284 nm (7,300). Melting point: > 250 °C.

$\{Pb(SC_6H_2$-2,4,6-$Cy_3)_2\}_2$ (**3**). 0.995 g (2.790 mmol) of HSC_6H_2-2,4,6-Cy_3 and 0.737 g (1.396 mmol) of $Pb(N(SiMe_3)_2)_2$ were combined in a 100 mL Schlenk flask and dissolved in hexane to give an orange solution. The flask was dried at *ca.* 40 °C under reduced pressure (*ca.* 0.01 torr) and the solvent was exchanged for toluene. Crystallization from slowly cooling a *ca.* 40 mL hot (*ca.* 100 °C) toluene solution gave 1.106 g (86.3 %) of **3** as orange X-ray quality single crystals.

^{1}H NMR (400 MHz, C_6D_6, 25 °C, δ/ppm): 7.15–6.99 (8H), 3.95 (8H), 2.51 (6H), 2.04–1.19 (120H). IR (Nujol, $\tilde{\nu}$/cm^{-1}): 2920 (s), 2840 (s), 1595 (w). 1550 (w), 1460 (s), 1450 (s), 1370 (m), 1345 (w), 1250 (s), 1085 (s), 1015 (s), 855 (m), 840 (w), 795 (s), 720 (w), 680 (w), 550 (w), 520 (w), 390 (w), 280 (w). UV–vis (λ/nm; ε/M^{-1}cm^{-1}): 284 (18,970), 413 (2,900). Melting point: >250 °C.

HSC_6H_2-2,4,6-Cy_3. 6.00 g (14.872 mmol) of BrC_6H_2-2,4,6-Cy_3[45] was added through a funnel to a 250 mL round-bottom Schlenk flask and *ca.* 150 mL of diethyl ether was added to create a colorless suspension of the bromide. The reaction flask was cooled to −25 °C and 18.8 mL of 1.7 M *t*-BuLi (2.15 equiv.) was added dropwise *via* cannula. After stirring at −25 °C for 2 h, the cold bath was removed, and the solution was warmed to room temperature. After 7 h of stirring at room temperature, the solvent was exchanged for *ca.* 150 mL of THF and 1.431 g (44.635 mmol) of crystalline sulfur were added *via* funnel in 3 portions to give a dark red solution. After stirring for 48 h at room temperature, the reaction mixture was cooled to −78 °C and 5.202 g (37.180 mmol) of Li[AlH_4] dissolved in Et_2O were added dropwise *via* cannula. The resultant yellow solution was stirred for 24 h and then quenched dropwise with deionized H_2O at 0 °C. Concentrated HCl was added dropwise until the pH of the solution became acidic. The organic and aqueous layers were separated with a separatory funnel and the aqueous layer was washed three times with *ca.* 100 mL portions of Et_2O. The organic layers were combined, dried with *ca.* 20 g of $MgSO_4$, and the solvent was removed using a rotary evaporator. The resultant yellow solid was redissolved in *ca.* 100 mL of boiling ethyl acetate and crystallized at room temperature to give 4.241 g (80.0 %) of colorless, air and moisture stable crystals of 2,4,6-tricyclohexylphenylthiol.

^{1}H NMR (600 MHz, $CDCl_3$, 25 °C, δ/ppm) 6.95 (2H), 3.08–3.06 (2H), 3.05 (1H, *H*SAr) 2.44 (1H), 1.89–1.25 (*ca.* 30H).

6. Computational details

Geometries of all studied systems were optimized in a solvent (SMD, benzene)[51] with dispersion corrected density functional theory, namely the PBE1PBE functional,[52–55] def2-TZVP basis sets,[56] and Grimme's D3 correction with Becke-Johnson damping,[57,58] using the Gaussian 16-C.01 program suite.[59] The structures were confirmed to be minima or transition states on the singlet potential energy hypersurface *via* calculation of the associated vibrational frequencies (all positive or one imaginary frequency, respectively).

CRediT authorship contribution statement

Connor P. McLoughlin: Data curation, Formal analysis, Investigation, Methodology, Supervision, Validation, Visualization, Writing – original draft, Writing – review & editing. **Anthony J. Witt:** Formal analysis, Investigation, Methodology, Validation. **Jonah P.D. Nelson:** Formal analysis, Software, Writing – original draft. **Heikki M. Tuononen:** Data curation, Formal analysis, Funding acquisition, Investigation, Software, Supervision, Writing – original draft, Writing – review & editing. **Philip P. Power:** .

Declaration of competing interest

The authors declare that they have no known competing financial interests or personal relationships that could have appeared to influence the work reported in this paper.

Data availability

Data will be made available on request.

Acknowledgments

C.P.M. would like to thank James C. Fettinger for his assistance with modeling the disorder present in complexes **1**–**3**. C.P.M. would also like to thank Dr. Ping Yu from the U.C. Davis NMR facility. We acknowledge the U.S. National Science Foundation (Grant No. CHE-2152760 to P.P. P.) and the University of Jyväskylä (H.M.T.) for funding.

Appendix A. Supplementary data

CCDC contains the supplementary crystallographic data for **1**–**4**, CCDC Accession numbers: 2294334-2294337. These data can be obtained free of charge via http://www.ccdc.cam.ac.uk/conts/retrieving.html, or from the Cambridge Crystallographic Data Centre, 12 Union Road, Cambridge CB2 1EZ, UK; fax: (+44) 1223-336-033; or e-mail: deposit@ccdc.cam.ac.uk. Spectroscopic (1H NMR, IR, and UV-Vis) data of 1–3, 1H-NMR data for 4, crystallographic tables for 1–4, and optimized structures (xyz-coordinates) (PDF). Supplementary data to this article can be found online at https://doi.org/10.1016/j.poly.2024.116877.

References

[1] D.H. Harris, M.F. Lappert, J. Chem. Soc., Chem. Commun. 21 (1974) 895–896.
[2] A. J. Veinot, D. L. Stack, J. A. C. Clyburne, J. D. Masuda, D. A. Dickie, U. Chadha, R A. Kemp, Inorg. Synth, 37 (2018), 1st Ed., Chapter 2, 26–31.
[3] T.J. Boyle, L.J. Tribby, L.A.M. Ottley, S.M. Han, Eur. J. Inorg. Chem. (2009) 5550–5560.
[4] H. Gerung, T.J. Boyle, L.J. Tribby, S.D. Bunge, C.J. Brinker, S.M. Han, J. Am. Chem. Soc. 128 (2006) 5244–5250.
[5] L. Wang, C.E. Kefalidis, T. Roisnel, S. Sinbandhit, L. Maron, J. Carpentier, Y. Sarazin, Organometallics 34 (2015) 2139–2150.
[6] B. Cetinkaya, I. Gumrukcu, M.F. Lappert, J.L. Atwood, R.D. Rogers, M. J. Zaworotko, J. Am. Chem. Soc. 102 (1980) 2088–2089.
[7] R. Kuriki, T. Kuwabara, Y. Ishii, Dalton Trans. 49 (2020) 12234–12241.
[8] C. Stanciu, A.F. Richards, M. Stender, M.M. Olmstead, P.P. Power, Polyhedron 25 (2006) 477–483.
[9] T. Hascall, A.L. Rheingold, I. Guzei, G. Parkin, Chem. Commun. (1998) 101–102.
[10] T. Hascall, K. Pang, G. Parkin, Tetrahedron 63 (2007) 10826–10833.
[11] B.G. McBurnett, A.H. Cowley, Chem. Commun. (1999) 17–18.
[12] G.D. Smith, P.E. Fanwick, I.P. Rothwell, Inorg. Chem. 29 (1990) 3221–3226.
[13] T.J. Boyle, T.Q. Doan, L.M. Steele, C. Apblett, S.M. Hoppe, K. Hawthorne, R. M. Kalinich, W.M. Sigmund, Dalton Trans. 41 (2012) 9349–9364.
[14] H. Yasuda, J. Choi, S. Lee, T. Sakakura, J. Organomet. Chem. 659 (2002) 133–141.
[15] W. Van Zandt, J.C. Huffman, J.L. Stewart, Main Group Met. Chem. 21 (1998) 237–240.
[16] C.S. Weinert, I.A. Guzei, A.L. Rheingold, L.R. Sita, Organometallics 17 (1998) 498–500.
[17] B.D. Rekken, T.M. Brown, M.M. Olmstead, J.C. Fettinger, P.P. Power, Inorg. Chem. 52 (2013) 3054–3062.
[18] C.S. Weinert, A.E. Fenwick, P.E. Fanwick, I.P. Rothwell, Dalton Trans. 4 (2003) 532–539.
[19] P.B. Hitchcock, M.F. Lappert, B.J. Samways, E.L. Weinberg, J. Chem. Soc., Chem. Commun. 24 (1983) 1492–1494.
[20] B. Kersting, B. Krebs, Inorg. Chem. 33 (1994) 3886–3892.
[21] B.D. Rekken, T.M. Brown, J.C. Fettinger, F. Lips, H.M. Tuononen, R.H. Herber, P. P. Power, J. Am. Chem. Soc. 135 (2013) 10134–10148.
[22] P.A.W. Dean, J.J. Vittal, N.C. Payne, Can. J. Chem. 63 (1985) 394–400.
[23] G. Barone, T.G. Hibbert, M.F. Mahon, K.C. Molloy, I.P. Parkin, L.S. Price, I. Silaghi-Dumitrescu, J. Chem. Soc., Dalton Trans. 23 (2001) 3435–3445.
[24] R.A. Shaw, M. Woods, J. Chem. Soc. A (1971) 1569–1571.
[25] W. Glegg, CCDC 1500411, CSD Communication (2016).
[26] G. Christou, K. Folting, J.C. Huffman, Polyhedron 3 (1984) 1247–1253.
[27] G.G. Briand, A. Decken, M.C. Finniss, A.D. Gordon, N.E. Hughes, L.M. Scott, Polyhedron 33 (2012) 171–178.
[28] Z.-G. Ren, X.-Y. Tang, L. Li, G.-F. Liu, H.-X. Li, Y. Chen, Y. Zhang, J.-P. Lang, Inorg. Chem. Comm. 10 (2007) 1253–1256.
[29] M. Charton, J. Am. Chem. Soc. 97 (1975) 1552–1556.
[30] B. Pinter, T. Fievez, F.M. Bickelhaupt, P. Geerlings, F. De Proft, Phys. Chem. Chem. Phys. 14 (2012) 9846–9854.
[31] S. Grimme, R. Huenerbein, S. Ehrlich, ChemPhysChem 12 (2011) 1258–1261.
[32] S. Rosel, J. Becker, W.D. Allen, P.R. Schreiner, J. Am. Chem. Soc. 140 (2018) 14421–14432.
[33] M. L. J. Wong, A. J. Sterling, J. J. Mousseau, F. Duarte, E. A. Anderson, Nat. Commun. 12 (2021) 1644/1–9.
[34] T. Kunz, C. Schrenk, A. Schnepf, Chem. Eur. J. 25 (2019) 7210–7217.
[35] M. Veith, P. Hobein, R. Rösler. Z. Naturforsch. 44b (1989) 1067−1081.
[36] A. Bondi, J. Phys. Chem. 68 (1964) 441–451.
[37] C.P. McLoughlin, D.C. Kaseman, J.C. Fettinger, P.P. Power, Dalton Trans. 52 (2023) 9582–9589.
[38] C.P. McLoughlin, J.C. Fettinger, P.P. Power, Inorg. Chem. 62 (2023) 10131–10140.
[39] P.B. Hitchcock, H.A. Jasim, R.E. Kelly, M.F. Lappert, J. Chem. Soc., Chem. Commun. 24 (1985) 1776–1778.
[40] C.S. Weinert, Main Group Met. Chem. 30 (2007) 93–100.
[41] A.L. Seligson, J. Arnold, J. Am. Chem. Soc. 115 (1993) 8214–8220.
[42] W. Wojnowski, M. Wojnowski, K. Peters, E.-M. Peters, H.G. von Schnering, Z. Anorg, Allg. Chem. 535 (1986) 56–62.
[43] A. Lorbach, A. Hübner, M. Wagner, Dalton Trans. 41 (2012) 6048–6063.
[44] P.P. Samuel, S. Kundu, C. Mohapatra, A. George, S. De, P. Parameswaran, H. W. Roesky, Eur. J. Org. Chem. 16 (2017) 2327–2331.
[45] L. Salvi, N.R. Davis, S.Z. Ali, S.L. Buchwald, Org. Lett. 14 (2012) 170–173.
[46] A.B. Pangborn, M.A. Giardello, R.H. Grubbs, R.K. Rosen, F.J. Timmers, Organometallics 15 (1996) 1518–1520.
[47] G. M. Sheldrick, SADABS, Siemens Area Detector Absorption Correction; Göttingen Universitat: Göttingen, Germany, (2008) 33.
[48] R.H. Blessing, Acta Cryst. Sect. a: Found. Cryst. 51 (1995) 33–38.
[49] G. M. Sheldrick, SHELXTL, Ver. 6.1; Bruker AXS: Madison, WI, 2002.
[50] O.V. Dolomanov, L.J. Bourhis, R.J. Gildea, J.A.K. Howard, H. Puschmann, J. Appl. Crystallogr. 42 (2009) 339–341.
[51] A.V. Marenich, C.J. Cramer, D.G. Truhlar, J. Phys. Chem. B 113 (2009) 6378–6396.
[52] J.P. Perdew, K. Burke, M. Ernzerhof, Phys. Rev. Lett. 77 (1996) 3865–3868.
[53] J.P. Perdew, K. Burke, M. Ernzerhof, Phys. Rev. Lett. 78 (1996) 1396.
[54] C. Adamo, V. Barone, J. Chem. Phys. 110 (1999) 6158–6170.
[55] M. Ernzerhof, G.E. Scuseria, J. Chem. Phys. 110 (1999) 5029–5036.
[56] F. Weigend, R. Ahlrichs, Phys. Chem. Chem. Phys. 7 (2005) 3297–3305.
[57] S. Grimme, J. Antony, S. Ehrlich, H. Krieg, J. Chem. Phys. 132 (2010) 154104.
[58] S. Grimme, S. Ehrlich, L. Goerigk, J. Comput. Chem. 32 (2011) 1456–1465.
[59] Gaussian 16, Revision C.01, M. J. Frisch, G. W. Trucks, H. B. Schlegel, G. E. Scuseria, M. A. Robb, J. R. Cheeseman, G. Scalmani, V. Barone, G. A. Petersson, H. Nakatsuji, X. Li, M. Caricato, A. V. Marenich, J. Bloino, B. G. Janesko, R. Gomperts, B. Mennucci, H. P. Hratchian, J. V. Ortiz, A. F. Izmaylov, J. L. Sonnenberg, D. Williams-Young, F. Ding, F. Lipparini, F. Egidi, J. Goings, B. Peng, A. Petrone, T. Henderson, D. Ranasinghe, V. G. Zakrzewski, J. Gao, N. Rega, G. Zheng, W. Liang, M. Hada, M. Ehara, K. Toyota, R. Fukuda, J. Hasegawa, M. Ishida, T. Nakajima, Y. Honda, O. Kitao, H. Nakai, T. Vreven, K. Throssell, J. A. Montgomery, Jr., J. E. Peralta, F. Ogliaro, M. J. Bearpark, J. J. Heyd, E. N. Brothers, K. N. Kudin, V. N. Staroverov, T. A. Keith, R. Kobayashi, J. Normand, K. Raghavachari, A. P. Rendell, J. C. Burant, S. S. Iyengar, J. Tomasi, M. Cossi, J. M. Millam, M. Klene, C. Adamo, R. Cammi, J. W. Ochterski, R. L. Martin, K. Morokuma, O. Farkas, J. B. Foresman and D. J. Fox, Gaussian, Inc.: Wallingford Connecticut, USA, 2016.